

# Hybrid Method for Numerical Implementation of Segmented Power Cable Conductors in Finite-element Based Ampacity Calculation

Henrik Strand<sup>1</sup>, Espen Eberg<sup>1</sup>, George J. Anders<sup>2</sup>

<sup>1</sup>*SINTEF Energy Research, Trondheim, Norway*

<sup>2</sup>*Technical University of Lodz, Poland*

## Abstract

This paper addresses challenges with modelling of segmented power cable conductors using finite element analysis (FEA) for ampacity calculation. Segmented conductors improve current distribution by minimizing skin and proximity effects, thus reducing conductor losses. 2D FEA simulation offers high flexibility and accuracy beyond IEC 60287 for complex laying geometries, but the modelling of losses in segmented constructions using FEA has proven difficult due to the big difference in wire size and twisting pitch, requiring great amounts of computational power. In this paper a hybrid method is proposed, in which the IEC 60287 empirical formulae for segmented conductors are included in a 2D FEA model. The proposed method shows a good correspondence to IEC standard calculations, with deviations in conductor AC resistance of less than 1 %.

## 1. Introduction

The increased implementation of renewable energy sources, combined with the increased demand for electric energy, calls for more efficient transmission of electric power using large cross-section power cables. Large, stranded cable conductors exhibit high losses due to skin and proximity effects. To improve the current distribution in the conductor, by minimizing skin and proximity effects, single wires, or segments of wires, in the conductor of power cables are often electrically insulated from each other into segmented conductors (see Figure 1). The name *Milliken conductor*, from a 20<sup>th</sup> century German engineer who invented it, is used in the standards to describe segmental construction.

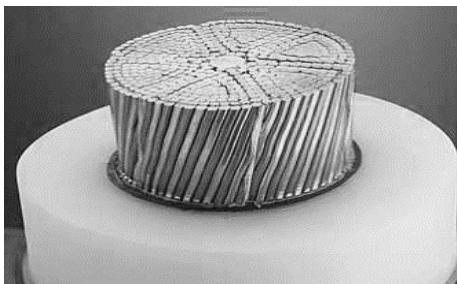


**Figure 1** - Example of segmented conductor construction with alternating bare and enamelled wires. Courtesy of Nexans.

State-of-the-art ampacity calculations employ the finite-element analysis (FEA) modelling due to high flexibility

in configurations and accuracy beyond IEC 60287 for complex laying geometries. But, due to the stranding and twisting of the wires and segments, as well as the difference in wire size and stranding pitch, modelling losses in such conductor designs using FEA models turns out to be a complex three-dimensional problem, requiring great amounts of computational power [1]. FEA-based ampacity calculations are thus usually based on replacing the segmented construction with a solid conductor of larger cross-section or increased conductivity, which causes loss of accuracy.

In this work a hybrid method where FEA modelling is combined with the empirical formulae in IEC 60287 describing segmented conductors is demonstrated. This keeps the potential flexibility and accuracy of FEA modelling but allows for more accurate ampacity calculation with segmented conductors.

## 2. Losses generated in a cable conductor

The current-carrying capacity of AC cables is strongly dependent on the losses in the conductor, which in turn is governed by its AC resistance at operating temperature. Under AC, the current is unevenly distributed in the conductor, due to the skin and the proximity effects.

The skin effect is the tendency of the current to distribute with a higher density near the surface of the conductor, flowing mainly at the "skin". This is caused by eddy currents cancelling the current near the centre of the conductor and adding to the current close to the surface as illustrated in Figure 2.

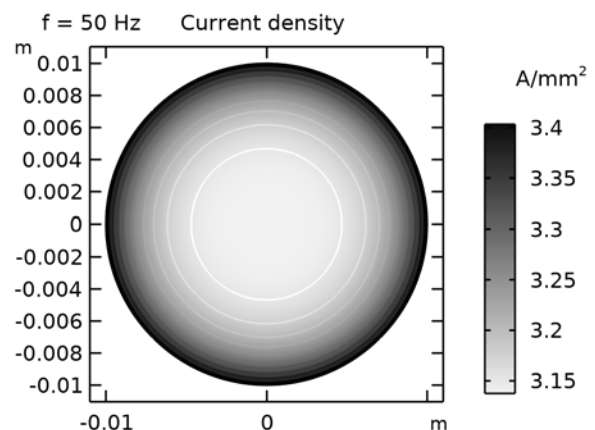


**Figure 2** - Plot of current density in single conductor when 50 Hz AC is applied of 1000 A.

The proximity effect is the tendency of the current to distribute along one side of the conductor when subjected to the magnetic fields of currents in adjacent conductors, as illustrated in Figure 3.

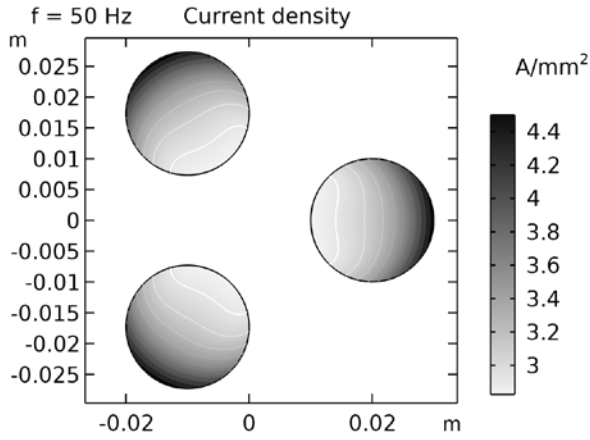


**Figure 3** - Current density plot (phasor magnitude peak values) in three conductors in triangular configuration when AC is applied at 50 Hz of 1000 A to each conductor.

To reduce the impact of these effects, segmented conductors have been introduced. Segmented conductors consist of segments of wires, electrically insulated from each other and twisted around the central axis. Additionally, in some segmental cable constructions, the wires themselves are enamelled, providing additional insulation between them. Segmental construction improves the conductor's current distribution, i.e., making it more homogeneous across the cross-section, thus reducing its AC resistance and increasing its total current-carrying capacity.

## 2.1. IEC standard method

The IEC 60287 standard [2] for calculating the current-carrying capacity of power cables, considers the contributions of skin and proximity effects by incorporating empirical skin and proximity effect factors  $y_s$  and  $y_p$  into the general formula for the conductor AC resistance:

$$R_{AC} = R_{DC}(1 + y_s + y_p) \quad (1)$$

where  $R_{DC}$  is the conductor DC resistance at operating temperature, given by:

$$R_{DC} = R_0(1 + \alpha_{20^\circ C}(T - 20^\circ C)) \quad (2)$$

where  $R_0$  is the conductor DC resistance at 20 °C,  $\alpha_{20^\circ C}$  is the temperature coefficient at 20 °C and  $T$  is the conductor operating temperature. The skin effect factor  $y_s$  is given by the following equations:

if  $0 < x_s \leq 2.8$ :

$$y_s = \frac{x_s^4}{192 + 0.8x_s^4} \quad (3)$$

if  $2.8 < x_s \leq 3.8$ :

$$y_s = -0.136 - 0.0177x_s + 0.0563x_s^3 \quad (4)$$

if  $x_s > 3.8$ :

$$y_s = 0.354x_s - 0.733 \quad (5)$$

where  $x_s$  is given by:

$$x_s^2 = \frac{8\pi f}{R_{DC}} 10^{-7} k_s \quad (6)$$

where  $f$  is the power line frequency (Hz) and  $k_s$  is the skin effect coefficient. Experimental values for  $k_s$  are given in IEC 60287-1-1 Table 2 [2].

The proximity effect factor  $y_p$  for three-core cables and for three single-core cables is given by the following equation:

$$y_p = \frac{x_p^4}{192 + 0.8x_p^4} \left( \frac{d_c}{s} \right)^2 \left[ 0.312 \left( \frac{d_c}{s} \right)^2 + \frac{1.18}{\frac{x_p^4}{192 + 0.8x_p^4} + 0.27} \right] \quad (7)$$

where  $d_c$  is the diameter of the conductor (mm),  $s$  is the distances between conductor axes (mm) and  $x_p$  is given by:

$$x_p^2 = \frac{8\pi f}{R_{DC}} 10^{-7} k_p \quad (8)$$

where  $f$  is the supply frequency and  $k_p$  is the proximity effect coefficient. Experimental values for  $k_p$  are given in IEC 60287-1-1 Table 2 [2].

The values of the skin and proximity effect coefficients  $k_s$  and  $k_p$  provided in the IEC standard are under consideration. These can be easily influenced by the conductor design, such as the condition of the strand insulation, which will have a great influence on the AC resistance. A set of modified  $k_s$  and  $k_p$  values, and a modified expression of  $y_s$ , is recommended in the CIGRE TB 727 [1]. Measurement methods are discussed in [1] and [3], and a common measurement method for the AC resistance of large cross-section conductors is under consideration. In this work, the  $k_s$  and  $k_p$  values given in IEC 60287 [2] are used.

## 2.2. FEA method

FEA simulations have been widely used for electromagnetic and thermal modelling of cable installations. The tool is usually applied to 2D geometries, where the cable components are represented as concentric cylindrical layers, assumed straight and parallel. In other words, 2D FEA simulations do not consider the helical twisting of components such as conductor strands and screen/armour wires, but only accounts for the effects of the transverse magnetic field,

neglecting the component parallel to the twisted strands or wires [4].

For a precise modelling of the electromagnetic effects in twisted and armoured power cables, authors in [5] and [6] claim that a 3D analysis is required. They propose a simplified 3D FEA method, in which a complete 3D model is shortened to its minimum length where the magnetic field periodicity still applies, achieving errors of below 10 % compared to a full-length model. In [7] authors claim that the maximum cable length solved by a FEA software in 3D is 3 m, however in [5] a 14 m cable was successfully modelled.

The examples above deal with the 3D modelling of losses in screen and armour wires in twisted cables. They do not treat the modelling of segmented conductors. Due to the stranding and twisting of the wires and segments in the core, combined with the big difference in wire size and twisting pitch, modelling losses in such conductor designs using FEA models turns out to be a complex three-dimensional problem with a very large mesh, requiring great amounts of computational power [1].

FEA methods provides large flexibility in geometries and dynamics in ampacity calculations. It would thus be beneficial to provide a simplified and applicable method for segmented conductors using FEA. To constrain computational cost/time to realistic levels, a method where 2D FEA modelling, imposing a homogeneous current distribution in the conductor, is combined with the IEC formulae for segmented conductors in order to consider the contributions from the skin and proximity effects, is proposed in the following.

### 3. Hybrid method

A hybrid method for numerical implementation of the segmented conductors in power cable ampacity calculations is proposed. In this work the method is implemented in the commercially available software COMSOL Multiphysics [8], but the approach is also applicable to other software with similar functionality. The method consists of the following steps:

1. Construct the cable geometry in 2D in FEA.
2. Impose a homogenous current distribution in the conductor. This is done by defining the conductor as a *homogenized multiturn coil*, a feature in which a domain is modelled as consisting of numerous tightly-wound conducting wires insulated from each other. Skin and proximity effects are thus neglected.
3. Use the IEC formulae to calculate  $R_{AC}$  (1), taking into account the skin and proximity effect factors  $J_s$  (3-5) and  $J_p$  (7).
4. Convert  $R_{AC}$  into an electrical conductivity  $\sigma_{AC}$ .
5. Apply the analytically calculated  $\sigma_{AC}$  to the homogenized multiturn conductor in the FEA model.

## 4. Comparison with the IEC Standard

To verify the proposed method, ampacity calculations have been conducted for an example cable with segmented conductor using the hybrid method and with the IEC standard calculations.

### 4.1. Model description

Table 1 gives the detailed description of the cable design used in this work. The cable has been modelled in both trefoil and flat formations, as shown in Figure 4 and Figure 5, respectively. Also, ampacities for both single-point (1-point) and solid (2-point) bonding have been calculated, giving four different configurations as summarized in Table 2. In Table 3 the installation parameters are presented.

**Table 1** - Cable description

Description	Cable 1
Voltage $U_0/U$ [kV]	76/132
Conductor material	Cu
Conductor design	Segmented insulated strands
Cross-section [ $\text{mm}^2$ ]	2000
Conductor diameter [mm]	56
Conductor DC resistance at 20 °C [ $\Omega/\text{km}$ ]	0.0090
$k_s$	0.35
$k_p$	0.20
Insulation	XLPE
Insulation diameter [mm]	86.4
Insulation thickness [mm]	13.1
Screen design	Cu wires + Al foil
Cross-section [ $\text{mm}^2$ ]	205 + 60
Screen diameter [mm]	95
Overall cable diameter [mm]	105

**Table 2** - Cable configurations

#	Formation	Bonding type
1	Trefoil	Single-point (1-pt)
2	Trefoil	Two-point (2-pt)
3	Flat	Single-point (1-pt)
4	Flat	Two-point (2-pt)

**Table 3** - Installation description

Description	Value
Soil thermal resistivity [ $\text{K}^*\text{m}/\text{W}$ ]	1
Depth of laying [m]	1
Ground temperature [ $^{\circ}\text{C}$ ]	20
Applied current [A]	800
Frequency [Hz]	50

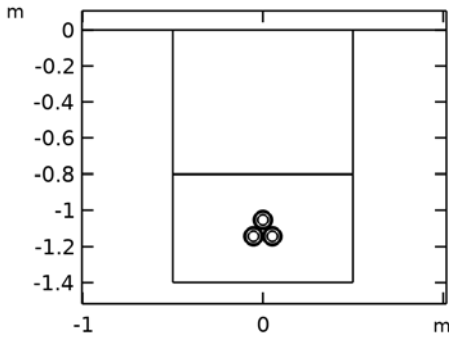


**Figure 4** – Cable installation in trefoil formation. The cables are enumerated in counterclockwise direction from the top.

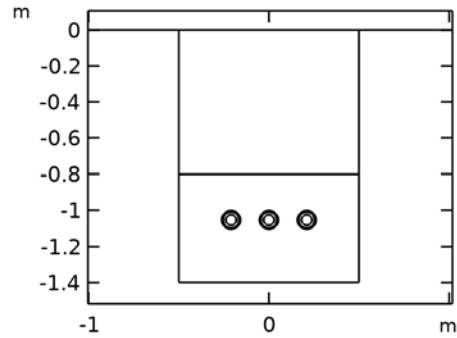


**Figure 5** - Cable installation in flat formation. The cables are enumerated from left to right

**4.2. Results and discussion**

The results from using the hybrid and the IEC methods are shown in Table 4. The deviation columns at the bottom represent the relative difference between the hybrid method and the IEC standard. The enumeration (1), (2) and (3) of the conductor and screen losses represent the different cables in the installation. The results are also presented in Figure 6 to Figure 9.

**Table 4** – Results comparison of hybrid method vs. IEC

		Hybrid method					
		Trefoil		Flat			
		1-pt	2-pt	1-pt	2-pt		
<b>Max. cond. temp.</b>	°C	34.6	60.5	31.8	74.7		
<b>Conductor R<sub>AC</sub></b>	μΩ/m	10.80	11.69	10.58	11.88		
<b>Cond. losses (1)</b>	W/m	6.93	7.47	6.70	7.60		
<b>Cond. losses (2)</b>	W/m	6.93	7.48	6.71	7.59		
<b>Cond. losses (3)</b>	W/m	6.93	7.48	6.70	7.49		
<b>Avg. cond. losses</b>	W/m	6.93	7.48	6.70	7.56		
<b>Screen losses (1)</b>	W/m	0.94	16.20	0.11	40.25		
<b>Screen losses (2)</b>	W/m	0.94	16.20	0.43	25.70		
<b>Screen losses (3)</b>	W/m	0.94	16.21	0.11	25.79		
<b>Avg. screen losses</b>	W/m	0.94	16.20	0.22	30.58		
		IEC standard					
		<b>Max. cond. temp.</b>	°C	35.8	60.4	32.3	78.3
		<b>Conductor R<sub>AC</sub></b>	μΩ/m	10.91	11.70	10.51	11.96
<b>Cond. losses (1)</b>	W/m	6.98	7.48	6.71	7.68		
<b>Cond. losses (2)</b>	W/m	6.98	7.48	6.72	7.66		
<b>Cond. losses (3)</b>	W/m	6.98	7.47	6.71	7.56		
<b>Avg. cond. losses</b>	W/m	6.98	7.48	6.71	7.63		
<b>Screen losses (1)</b>	W/m	0.82	15.12	0.09	44.20		
<b>Screen losses (2)</b>	W/m	0.82	15.12	0.39	25.80		
<b>Screen losses (3)</b>	W/m	0.82	15.13	0.10	29.40		
<b>Avg. screen losses</b>	W/m	0.82	15.12	0.19	33.13		
		Deviation					
		<b>Max. cond. temp</b>	%	-3.35	0.17	-1.55	-4.60
		<b>Conductor R<sub>AC</sub></b>	%	-0.97	-0.13	0.71	-0.69
		<b>Avg. cond. losses</b>	%	-0.72	-0.01	-0.15	-0.96
<b>Avg. screen losses</b>	%	14.72	7.14	11.93	-7.70		

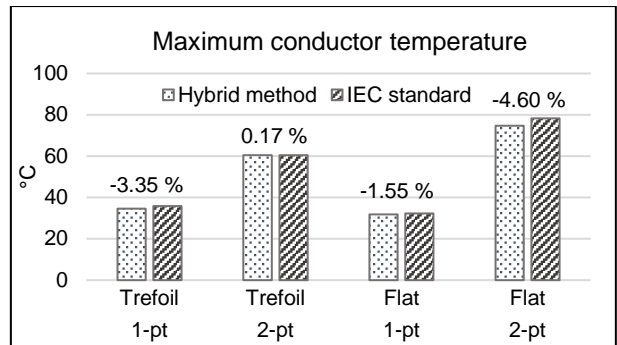


**Figure 6** - Maximum conductor temperature. Hybrid method vs. IEC. Deviation in % for each modelled configuration. In flat formation, the middle cable (cable 2) is considered.

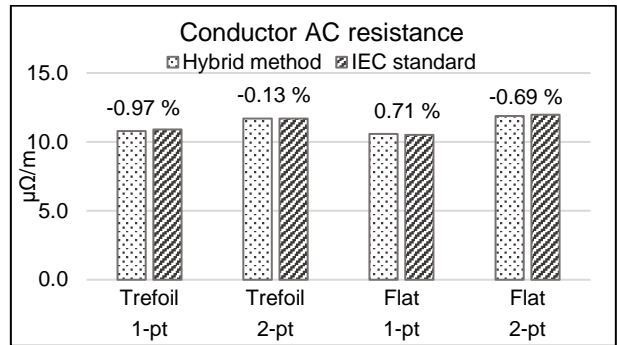


**Figure 7** - Conductor AC resistance at operating temperature. Hybrid method vs. IEC. Deviation in % for each modelled configuration. The resistances are calculated using the maximum conductor temperatures from Table 4. In flat formation, the middle cable (cable 2) is considered.

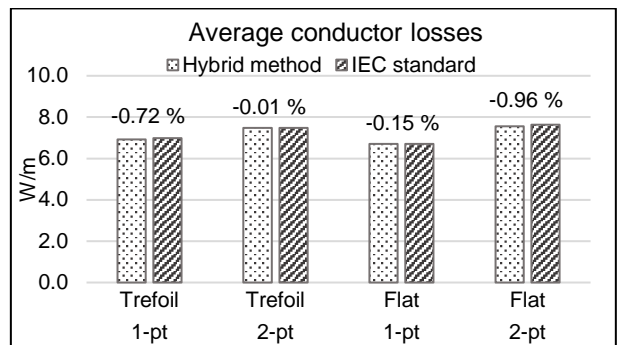


**Figure 8** - Average conductor losses. Hybrid method vs. IEC. Deviation in % for each modelled configuration.

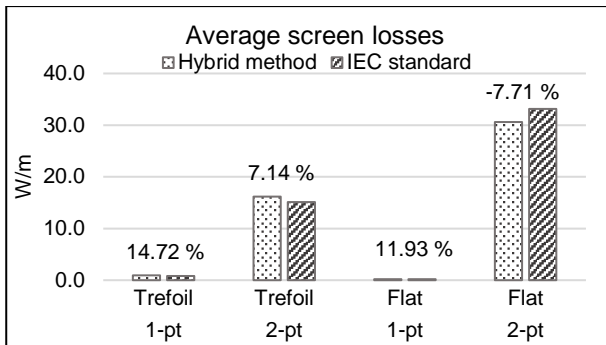


**Figure 9** - Average screen losses. Hybrid method vs. IEC. Deviation in % for each modelled configuration.

Overall, the results from using the hybrid method match well with those from using the IEC standard. The hybrid method gives a maximum conductor temperature in trefoil formation 2-pt bonding of 60.5 °C, which is only 0.1 °C higher than the value found using IEC, giving a relative difference of 0.17 %. The highest deviation of conductor temperature is -4.60 %, which is found for flat formation 2-pt bonding.

The relative differences with regards to conductor AC resistance  $R_{AC}$  are very small, all below 1 %. The same can be said about the relative differences of the average conductor losses, which range from -0.01 % to -0.96 %. This indicates that the hybrid method for modelling of segmented conductors works well compared to the IEC analytical calculations. Nevertheless, the deviations in conductor resistance and losses are small, but not zero. These small differences could be due to the variation in conductor temperature at which the AC resistance is computed.

We also see that even though the relative differences in screen losses for the 1-pt bonding cases are big (14.72 % and 11.93 %, respectively), the absolute differences are very small (0.12 W/m and 0.03 W/m). This means that the deviation in screen losses contributes little to the total temperature rise in the cable.

The deviation of -4.60 % in conductor temperature for the flat formation 2-pt bonding is, however, probably due to the screen losses, which increase in 2-pt bonded cables due to the presence of circulating currents. The average screen losses in flat formation 2-pt bonded are 7.7 % lower with the hybrid method than with IEC, which is unexpected. This needs further investigation and should be the subject of future work.

## 5. Conclusion

The primary goal of this work was to develop a simplified and practical method for implementing segmented conductors in 2D FEA based power cable ampacity calculations. The model should accurately reproduce the losses in the conductor compared to IEC standard calculations, while preserving the flexibility of FEA with regards to complex laying geometries.

The main conclusions that can be drawn from the analysis of this paper are the following:

- The proposed method consists of a hybrid between a FEA based cable model and the IEC standard formulae for Milliken conductors.
- The results of the proposed method match up well with the IEC standard, with relative differences in both  $R_{AC}$  and conductor losses of less than 1 %.
- The relative difference in maximum conductor temperature in 2-pt bonding is most likely not due to the modelling of the segmented conductor itself, but rather the losses in the screen. This needs further investigation.

## 8. References

- [1] CIGRE Working Group B1.03, *TB 272 - Large cross-sections and composite screen designs*. 2005.
- [2] International Electrotechnical Commission, *IEC 60287 Part 1-1: Electric cables: Calculation of the current rating*. 2014.
- [3] R. Suchantke, 'Alternating Current Loss Measurement of Power Cable Conductors with Large Cross Sections Using Electrical Methods', Technische Universität Berlin, 2018.
- [4] B. Gustavsen, M. Hoyer-Hansen, P. Triverio, and U. R. Patel, 'Inclusion of Wire Twisting Effects in Cable Impedance Calculations', *IEEE Trans. Power Deliv.*, vol. 31, no. 6, pp. 2520–2529, Dec. 2016.
- [5] J. del-Pino-López, M. Hatlo, and P. Cruz-Romero, 'On Simplified 3D Finite Element Simulations of Three-Core Armored Power Cables', *Energies*, vol. 11, no. 3081, Nov. 2018.
- [6] J. C. del-Pino-López and P. Cruz-Romero, 'Experimental validation of ultra-shortened 3D finite element electromagnetic modeling of three-core armored cables at power frequency', *Electr. Power Syst. Res.*, vol. 203, no. 107665, Feb. 2022.
- [7] R. Benato, S. Dambone Sessa, and M. Forzan, 'Experimental Validation of Three-Dimension Multiconductor Cell Analysis by a 30 km Submarine Three-Core Armoured Cable', *IEEE Trans. Power Deliv.*, vol. 33, no. 6, pp. 2910–2919, Dec. 2018.
- [8] *COMSOL Multiphysics® v.6.0*. Stockholm, Sweden: COMSOL AB, 2022. [Online]. Available: <https://www.comsol.com>